J Appl Electrochem (2009) 39:321–327
DOI 10.1007/s10800-008-9674-4

ORIGINAL PAPER

Electrocatalytic reduction of hydrogen peroxide at nanostructured copper modified electrode

Thangavelu Selvaraju · Ramasamy Ramaraj

Received: 5 April 2008 / Accepted: 29 September 2008 / Published online: 18 October 2008

Abstract The electrocatalytic reduction of hydrogen peroxide (H_2O_2) has been studied at nanostructured copper (Cu_{nano}) modified glassy carbon (GC/Cu_{nano}) electrode in phosphate buffer (pH 7.2). The electrical properties of GC/Cu_{nano} modified electrodes were studied by electrochemical impedance spectroscopy (EIS). Surface and electrochemical characterization were carried out by using atomic force microscopy (AFM) and cyclic voltammetry. A well-defined H_2O_2 reduction signal, which is due to mediation of a surface active site redox transition exhibits at the GC/Cu_{nano} electrode. The Cu_{nano} is acting as a bridge without the aid of any other electron mediator, which enables the direct electron transfer between the modified electrode and the substrate. The results are compared with bulk copper macroelectrode and emphasized the efficiency of the Cu_{nano} modified electrode. Systematic investigations were made to optimize the experimental parameter, such as applied potential (E_{app}) for copper electrodeposition. The calibration curve obtained from chronoamperometric studies was found to be linear in the range 0.5 to 8.0 μM H_2O_2 with a detection limit of ca.10 nM (S/N = 3) at the GC/Cu_{nano} electrode. The modified electrode is stable for 1 week in phosphate buffer after repetitive measurements.

Keyword Nanostructured copper · Modified electrode · Hydrogen peroxide · Electrocatalysis · Sensors

T. Selvaraju · R. Ramaraj (✉)
Centre for Photoelectrochemistry, School of Chemistry, Madurai Kamaraj University, Madurai 21, India
e-mail: ramarajr@yahoo.com

1 Introduction

The assembly of metal nanoparticles into ordered two-dimensional and three-dimensional superstructures has become an interesting aspect in sensors, catalysis, etc. [1–9]. To realize such nanostructures-based materials, it is necessary to design some methods to orient and integrate the nanomaterials in the surface-confined device architecture. The nanosized metal particles mediate the chemical reaction and provide better electrocatalytic activity in chemical sensor applications. A metal complex attached on the surface of the electrode using an irreversibly adsorbed ligand has been explored for the purpose of electrocatalytic reduction of H_2O_2 [10–12], which is fundamentally important for low-cost catalyst development in energy devices such as fuel cells. To increase the robustness and durability, a variety of electrode materials, such as graphite carbon paste, polypyrrole, sol–gel and prussian blue and mediators suitable for peroxidase-based electrodes have been reported [13–17]. Nevertheless, the stability and fouling of the materials is a serious problem in using these electrodes [18, 19]. Most of the mediators and metal complexes are unstable at higher pH and hence have a limited working pH range. The H_2O_2 biosensor based on horseradish peroxidase immobilized on colloidal gold was found to be electrocatalytically active in the reduction of H_2O_2 without using an electron transfer mediator [20]. As this method has paved the way for the construction of third generation mediator-free chemical sensor and there has been considerable interest in fabricating H_2O_2 sensor based on metal nanoparticles modified electrodes [18, 21–29]. Modification of carbon electrode with conductive metallic oxides was reported earlier [29, 30].

Electrochemical investigations of H_2O_2 reduction using polycrystalline copper electrode have been documented

[30–32]. The importance of H_2O_2 in the overall reduction mechanism of oxygen on copper electrode was pointed out in the early work of Delahay [33]. The convenience of studying the electrochemical behavior of H_2O_2 in the absence of oxygen for understanding the overall reduction of H_2O_2 at corroding metals has been stressed previously [34]. However, so far this property has rarely been used for analytical applications. Recently, copper electrochemistry has been studied and summarized [35], which shows that a surface activated copper might play an important role in the electrocatalysis of organic compounds. This work deals with the fabrication a high precision and inexpensive analytical method for the electrocatalytic reduction of H_2O_2. In the present study, we first illustrate the preparation of nanostructured copper on glassy carbon electrode followed by measuring its impedance changes. Then, we present the electrocatalytic phenomena of this modified electrode to assess the amplified current signal and the result was compared to bulk copper electrode.

2 Experimental

All chemicals were of analytical-reagent grade from Merck. Fresh solution of H_2O_2 was prepared in the working buffer and stored in dark at <4 °C. Copper sulphate, sodium perchlorate, monosodium and disodium hydrogen phosphate (Merck) were used as received. 0.1 M phosphate buffer (pH 7.2) was used in the experiment. All aqueous solution has been prepared in de-ionized double distilled water. When anaerobic conditions were chosen, purified nitrogen gas was used to expel the dissolved oxygen.

All the electrochemical experiments were performed in an EG&G PAR model 283 potentiostat/galvanostat controlled by Echem software loaded personnel computer. The electrochemical measurements were carried out in a two-compartment three-electrode system consists of a platinum wire as the counter electrode, standard calomel electrode as the reference electrode and glassy carbon (GC) as the working electrode (0.07 cm^2). The electrochemical impedance spectroscopy (EIS) analyses were performed using CHI 650B potentiostat (CH Instruments, Inc., TX, USA). The surface image of nanostructured copper was studied on Indium Tin Oxide (ITO) electrode. The surface images of copper macroelectrode and nanostructured copper were measured by atomic force microscopy (AFM) using the Shimadzu SPM 9500 scanning probe microscope (AFM analysis) with Nanoscope IIIa controller. The gold cantilever diameter in AFM measurement is 50 μm.

The nanostructured copper (Cu_{nano}) was deposited electrochemically on GC electrode using a solution of 0.01 M $CuSO_4$ and 0.1 M $NaClO_4$ at an applied potential of −0.4 V(SCE). For comparison, nanostructured copper was deposited at different applied potential between −0.1 and −0.6 V(SCE). Under these conditions, the charge consumed during nanostructured copper loading was calculated as 0.011 C cm^{-2}. Prior to every experiment, the electrodes were polished with an aqueous suspension of 1.0 and 0.05 μm alumina on a Buehler cloth, rinsed copiously with doubly distilled water and sonicated in a water bath for 3 min followed by activation to remove the charging current.

3 Results and discussion

3.1 Surface analysis of bulk copper and ITO/Cu_{nano} electrodes by atomic force microscopy (AFM)

Figure 1 shows the AFM images of bulk copper (copper macroelectrode) and ITO/Cu_{nano} electrodes. The AFM image of a bulk copper has been recorded (Fig. 1a) to compare its morphology and roughness with the surface of ITO/Cu_{nano} electrode (Fig. 1b). The bulk copper electrode depicts no characteristic observation compared to ITO/Cu_{nano} electrode. Two-dimensional AFM image of ITO/Cu_{nano} electrode (Cu_{nano} electrodeposited at −0.4 V) is shown in Fig. 1b. It clearly emphasized many spherical Cu_{nano} have formed on the ITO surface. The diameter of the spherical nanostructures is in the range of 50–150 nm. As shown in Fig. 1b, a high-coverage of non aggregated Cu_{nano} was observed. Figure 1c shows the three-dimensional AFM image of nanostructured copper on the electrode surface. The average grain size is about 95 nm with a roughness factor of 92.74 nm (Rq) which is confirmed in the cursor plot (Fig. 1d) acquired from Fig. 1c. The particle size is not precise apparently due to the surface oxides which are known for their ability to destabilize particle size and other properties [36, 37]. The electrodeposition of copper at −0.4 V leads to the formation of nanostructured copper with homogeneous distribution on the electrode surface and majority of structures remains close to adjacent ones.

3.2 Electrochemical impedance spectroscopy (EIS)

EIS is used to investigate the impedance changes at the Cu_{nano} modified electrode. It is an effective electrochemical technique for probing the features of surface modified electrodes [38, 39]. EIS measurements have been performed to characterize the interfacial properties of bulk copper electrode, bare glassy carbon electrode (GC) and nanostructured copper modified GC electrode (GC/Cu_{nano}) (Cu_{nano} was electrodeposited at −0.4 V). Figure 2 shows the Nyquist plot of the EIS for bulk copper electrode, bare GC and GC/Cu_{nano} electrode in the presence of equimolar $[Fe(CN)_6]^{3-/4-}$ in 0.1 M phosphate buffer. The

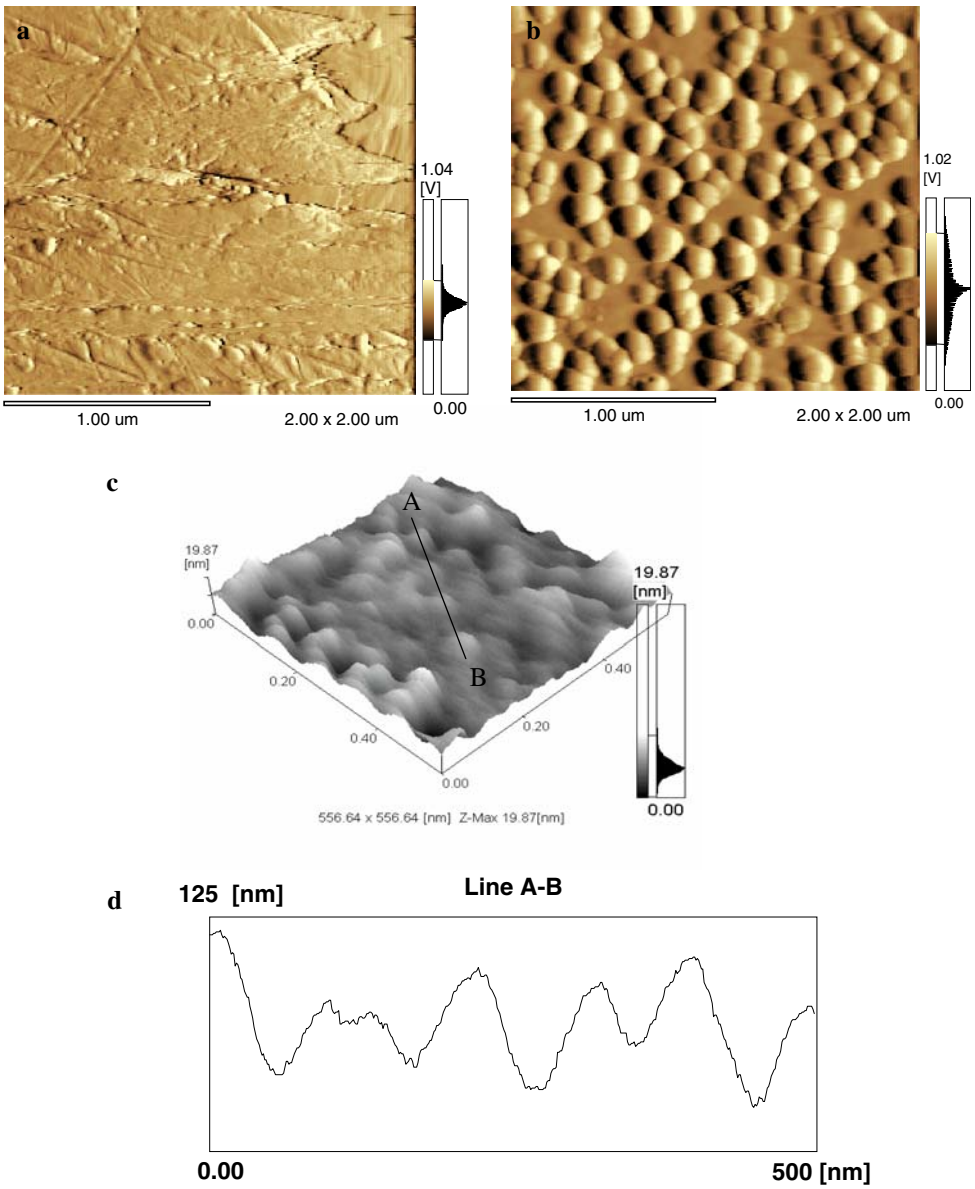

Fig. 1 Tapping mode of two-dimensional AFM images of bulk Cu electrode (**a**), ITO/Cu_{nano} electrode (**b**) and three-dimensional AFM image of ITO/Cu_{nano} electrode (**c**). (Cu_{nano} electrodeposited at −0.4 V (SCE)). Cursor plot (**d**) was obtained for the line A–B shown in Fig. 1c

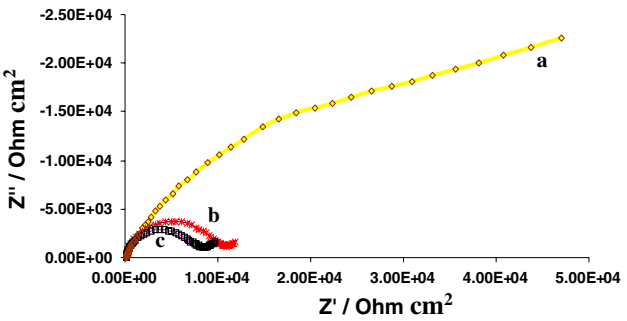

Fig. 2 Electrochemical impedance spectra of (**a**) bulk Cu, (**b**) bare GC and (**c**) GC/Cu_{nano} electrodes in 0.1 M phosphate buffer (pH 7.2) and 1 mM $K_3[Fe(CN)_6]/K_4[Fe(CN)_6]$. Applied potential: 0.2 V and frequency range: 1 Hz–100 kHz

perturbation voltage was 0.2 V and the frequency range was 1 Hz–100 KHz. The semicircle diameter equals the charge transfer kinetics of the redox-probe at the electrode interface, where Z_{re} and Z_{im} are real and imaginary parts of impedance (Z). As shown in curve a, a very large charge transfer resistance (R_{ct}) was observed for $[Fe(CN)_6]^{3-/4-}$ couple at bulk copper electrode (Cu wire, diameter 0.3 cm). The pretreated bare GC and GC/Cu_{nano} electrodes showed a decreased R_{ct} of 12 KΩ cm^2 (curve b) and 8 KΩ cm^2 (curve c), respectively. The semicircle plot is probed by higher frequencies, which means that the dynamics of electron transfer in higher frequency range is observed and the current due to voltage excitation is under kinetic control. The low frequency region, where the slope of Z_{re} vs.

Z_{im} is unity, is dominated by mass region [40]. It could be observed that the diameter of the semicircle plot was decreased with the modified process of the GC electrode. The semicircle of curve b was remarkably smaller than curve a. This obvious change indicates the pretreated GC electrode accelerates electron transfer of the probe molecule. The semicircle of curve c was even smaller that the nanostructured copper facilitated the electron-transfer process on the electrode surface. Hence, it is clear that the GC/Cu_{nano} modified electrode is more suitable for electrochemical sensing due to its smaller electron transfer resistance. It is consistent with the cyclic voltammetry results obtained toward H_2O_2 reduction (*vide infra*).

3.3 Electrocatalytic reduction of H_2O_2 at GC/Cu_{nano} electrode

The bare GC electrode shows no characteristic behavior between 0.8 and −0.8 V in the presence of H_2O_2 in 0.1 M phosphate buffer (pH 7.2) (Fig. 3a). This phenomenon interprets that H_2O_2 reduction could not be achieved at bare GC electrode. Figure 3b and c show the cyclic voltammograms of GC/Cu_{nano} electrode (electrodeposited at −0.4 V) in the absence and presence of H_2O_2 in 0.1 M phosphate buffer. A cathodic peak (Fig. 3b) at −0.28 V due to $Cu^{I}O$ reduction to Cu^0 and an anodic peak at −0.08 V due to Cu^0 oxidation were observed at GC/Cu_{nano} electrode. The presence of copper and copper oxides on the surface of the electrode was confirmed by cyclic voltammetric result [41]. Our interest is to utilize this nanostructured copper electrode in the electrocatalytic application.

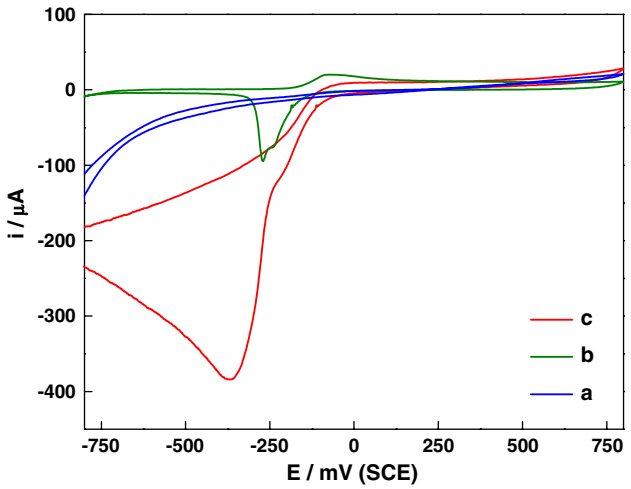

Fig. 3 CV recorded for 9×10^{-5} M H_2O_2 in 0.1 M phosphate buffer at bare GC electrode (**a**). CVs recorded at GC/Cu_{nano} electrode in the absence (**b**) and presence (**c**) of 9×10^{-5} M H_2O_2 in 0.1 M phosphate buffer (Cu_{nano} electrodeposited at −0.4 V). Scan rate = 50 mVs^{-1}

In the presence of H_2O_2, GC/Cu_{nano} electrode shows a remarkably enhanced reduction peak current starting from −0.1 V (Fig. 3c). This indicates that the H_2O_2 reduction could be observed at the GC/Cu_{nano} electrode. In the GC electrode, Cu_{nano} mediates the direct electron transfer leading to the H_2O_2 reduction and improved its electrocatalytic activity at this modified electrode. The H_2O_2 reduction peak has been observed at −0.3 V (Fig. 3c) which follows a two-electron and two-proton reaction (Eq. 1) [18].

$$H_2O_2 + 2H^+ + 2e^- \xrightarrow{Cu^0} 2H_2O \quad (1)$$

When compared to earlier reports on H_2O_2 reduction at different electrodes [10–12, 20], it is apparent that overpotential has decreased by about 100–400 mV. In addition, H_2O_2 reduction current is also enhanced at the GC/Cu_{nano} electrode which shows Cu_{nano} acts as the catalytic center and mediates the reaction. The absence of specific peak in the anodic scan indicates that the H_2O_2 oxidation is not a favorable reaction at the GC/Cu_{nano} electrode. In this system, the nanostructured copper exhibits a metastable active surface redox transition, which is of major impact in both electrocatalytic and electrodeposition viewpoint [42]. In addition, the nature of this transition is not well understood and it apparently functions as redox mediator [43, 44], which dominates in the electrocatalytic behavior of this electrode system. It is worth mentioning here that, despite extensive worldwide investigation, the chemical behavior of surface active sites in general is not well established and is largely a matter of speculation. Active state behavior of metal surface is very difficult to investigate as the species involved are of quite low coverage and unstable (or metastable).

3.4 Influence of E_{app} on the electrodeposition of Cu_{nano} and its effect on H_2O_2 reduction

Copper was electrochemically deposited on the GC electrode by using 0.01 M $CuSO_4$ and 0.1 M $NaClO_4$ at different applied potential (E_{app}) ranging from 0.0 to −0.6 V(SCE). Under these conditions, the charge consumed during Cu_{nano} deposition was measured as 0.011 C cm^{-2}. It means that the modified electrodes should maintain its charge consumption with respect to different E_{app} towards nanostructure formation. In order to analyze the electrocatalytic activity of metastable active state in nanostructured copper electrode, the charge has been maintained during electrodeposition at different E_{app}. The GC/Cu_{nano} electrodes were prepared at different E_{app} such as 0, −0.1, −0.2, −0.3, −0.4, −0.5 and −0.6 V. The above prepared electrodes were used to record cyclic voltammogram in the presence of 0.13 mM H_2O_2 in 0.1 M phosphate

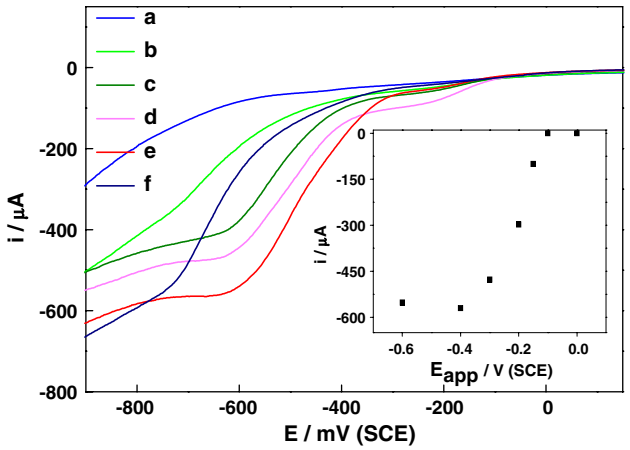

Fig. 4 Linear sweep voltammograms (LSVs) recorded at GC/Cu_{nano} electrode in the presence of 0.13 mM H_2O_2 in 0.1 M phosphate buffer. GC/Cu_{nano} electrode was prepared at different E_{app} (a = 0, b = −0.1, c = −0.2, d = −0.3, e = −0.4 and f = −0.5 V). Scan rate = 50 mV s^{-1}. Inset: Effect of different E_{app} on the formation of Cu_{nano} on GC electrode (GC/Cu_{nano}) and the corresponding reduction peak current of 0.13 mM H_2O_2 in 0.1 M phosphate buffer

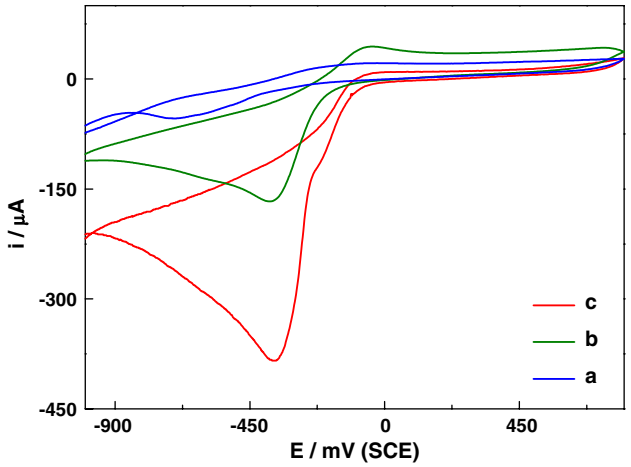

Fig. 5 CVs recorded at bulk Cu electrode in the absence (**a**) and presence (**b**) of 9×10^{-5} M H_2O_2 and at GC/Cu_{nano} electrode in the presence (**c**) of 9×10^{-5} M H_2O_2 in 0.1 M phosphate buffer (Cu_{nano} electrodeposited at −0.4 V). Scan rate = 50 mV s^{-1}

buffer. Figure 4 shows the linear sweep voltammetric responses observed for 0.13 mM H_2O_2 at GC/Cu_{nano} electrode which prepared in different E_{app}. An increase in the H_2O_2 reduction peak current was observed at GC/Cu_{nano} electrode which prepared in different E_{app} between 0 and −0.6 V and reached a maximum electrocatalytic activity for the nanostructured copper prepared at −0.4 V (Fig. 4e). The cathodic peak current observed for H_2O_2 reduction were plotted against E_{app} as shown in Fig. 4 (inset). An increase in the electrocatalytic H_2O_2 reduction peak current was observed at the GC/Cu_{nano} electrodes prepared at more negative potential and attained maximum at −0.4 V as shown in Fig. 4(inset). The GC/Cu_{nano} electrodes prepared between 0 and −0.4 V show a significant difference in the electrocatalytic behavior (Fig. 4) whereas saturation might be taking place during nanostructued copper deposited at more negative E_{app} such as −0.6 V, etc. On the other hand, the electrocatalytic H_2O_2 oxidation was not observed at the GC electrode. In our earlier report, we explained the deposition of copper structures with respect to different E_{app} and explained the importance of copper deposition at more negative potential [45].

3.5 Comparative study of H_2O_2 reduction at bulk copper and GC/Cu_{nano} electrode

Figure 5a shows the cyclic voltammogram recorded at bulk copper (copper macroelectrode) in deaerated 0.1 M phosphate buffer. The copper oxide growth appeared at potential positive to −0.25 V underwent reduction at more negative potential in the cathodic scan as shown in Fig. 5a.

Figure 5b shows the cyclic voltammogram recorded at bulk copper electrode for 9×10^{-5} M H_2O_2 in 0.1 M phosphate buffer. An increase in the peak current was observed due to H_2O_2 reduction at the bulk copper electrode (Fig. 5b). Figure 5c shows the cyclic voltammogram recorded at the GC/Cu_{nano} electrode for 9×10^{-5} M H_2O_2 in 0.1 M phosphate buffer. It is evident that the GC/Cu_{nano} electrode shows higher catalytic current compared to bulk copper electrode towards H_2O_2 reduction.

3.6 Constant potential amperometric studies

Chronoamperometry is also used to test the applicability of the GC/Cu_{nano} modified electrode for the determination of H_2O_2. The nanostructured copper electrodeposited at −0.4 V on GC electrode was used as a transducer for the electrocatalytic reduction of H_2O_2. Figure 6a shows the chronoamperogram that was recorded at the GC/Cu_{nano} electrode in a continuously stirred 0.1 M phosphate buffer (pH 7.2) at an operating potential of −0. 5 V. As shown in Fig 6a, during successive additions of 0.5 μM H_2O_2 at a sampling time of ca. 3 s, a well-defined response was obtained. Figure 6a shows the chronoamperogram recorded in the concentration range between 0.5 and 8 μM H_2O_2 and corresponding increase in the peak current. Figure 6b depicts that the current varies linearly with the concentration of H_2O_2 in the range from 0.5 to 8 μM. The sensitivity was found to be ∼1.1 μA/μM and the detection limit was calculated based on the $3\sigma/m$ criterion, where σ and m represents the blank standard deviation and sensitivity respectively. The detection limit was found to be 10 nM. The response time at each addition of H_2O_2 is 3 s, which indicates a fast electron transfer process at this modified

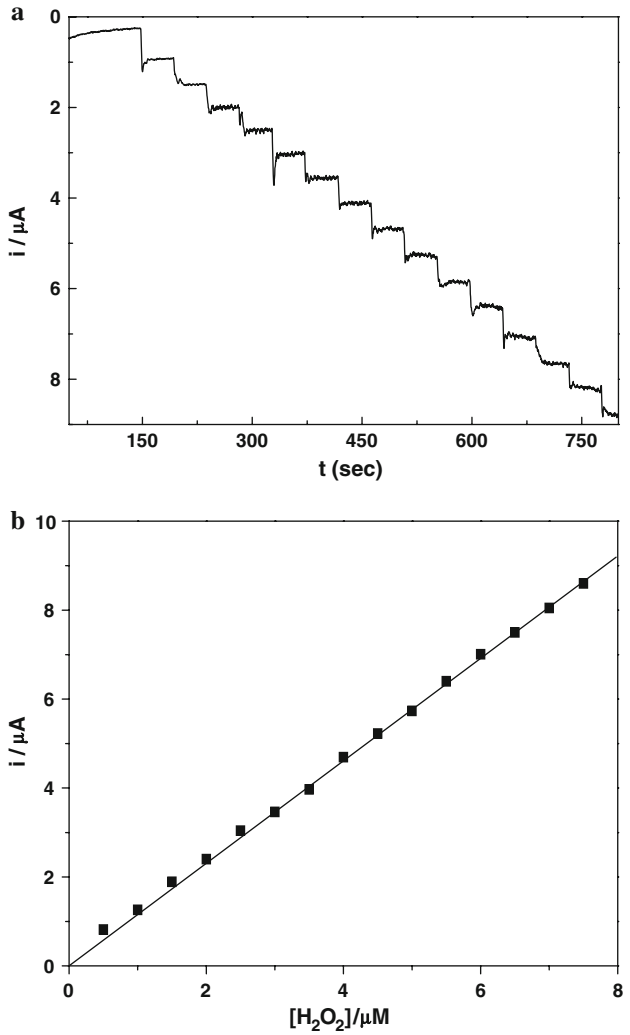

Fig. 6 (**a**) Current–time response observed for H_2O_2 at the GC/Cu_{nano} electrode after subsequent spiking of 0.5 μM H_2O_2. (**b**) Calibration plot observed for H_2O_2 at an applied potential of −0.5 V(SCE) in 0.1 M PBS

electrode. The electrode was fairly stable for 1 week when stored at room temperature in phosphate buffer after repetitive measurements and 95% reproducibility was achieved at the GC/Cu_{nano} electrode.

4 Conclusions

A simple and robust nanostructured copper modified electrode (GC/Cu_{nano}) was prepared by electrochemical method. The cyclic voltammetric results confirm the presence of electrodeposited copper on the GC electrode surface. The size and uniformity of the nanostructured copper were characterized by AFM. In addition, the electrical properties of the Cu_{nano} modified electrode were analyzed by EIS. The electrochemical studies showed that the Cu_{nano} electrodeposited at −0.4 V is an excellent electrocatalyst for the reduction of H_2O_2 in submicromolar concentration. Cu_{nano} exhibits an active surface redox transition, which is of major significance in the electrocatalytic reduction of H_2O_2. Finally, the sensitivity and the detection limit of H_2O_2 were highlighted.

Acknowledgements RR acknowledges the Department of Science and Technology (DST) and Council of Scientific and Industrial Research (CSIR), New Delhi for financial support. TS is a recipient of CSIR-SRF fellowship.

References

1. Ball P (1993) Nature 362:123
2. Wieckowski A, Savinova ER, Vayenas CG (eds) (2003) Catalysis and electrocatalysis at nanoparticle surfaces. Marcel Dekker, New York
3. Peschel S, Schmid G (1995) Angew Chem Int Ed Engl 34:1442
4. Andres RP, Bielefeld JD, Henderson JI, Janes DB, Kolagunta VR, Kubiak CP, Manoney W, Osifchin RG (1996) Science 273:1690
5. Hrapovic S, Luong JHT (2003) Anal Chem 75:3308
6. Male KB, Hrapovic S, Liu Y, Wang D, Luong JHT (2004) Anal Chim Acta 516:35
7. Lewis LN (1993) Chem Rev 93:2693
8. Cho GL, Lakshmi BB, Fischer ER, Martin CR (1998) Nature 393:346
9. Pei J, Li XY (1998) J Electroanal Chem 441:245
10. Shi C, Anson FC (1990) Inorg Chem 29:4298
11. Winter M, Brodd RJ (2004) Chem Rev 104:4245
12. Welch CM, Banks CE, Simm AO, Compton RG (2005) Anal Bioanal Chem 382:12
13. Razumas J, Kazlauskaite R, Vidziunaite R (1996) Bioelectrochem Bioeng 39:139
14. Luovich V, Sheeline A (1997) Anal Chem 69:454
15. Navaz Diaz A, Ramos Peinado MC, Torijas Minguez MC (1998) Anal Chim Acta 363:221
16. Karyakin AA, Gitlemacher OV, Karyakina EE (1995) Anal Chem 67:2419
17. Ghosh PK, Mau AW-H, Bard AJ (1984) J Electroanal Chem 169:315
18. Cai LT, Chen HY (1999) Sens Actuators B 55:14
19. Scharf U, Grabner EW (1996) Electrochim Acta 41:233
20. Hill HAO (1996) Coord Chem Rev 151:115
21. Wang J, Musameh M, Lin Y (2003) J Am Chem Soc 125:2408
22. Delvaux M, Walcarius A, Champagne SD (2004) Anal Chim Acta 525:221
23. Li X, Heryadi D, Gewirth AA (2005) Langmuir 21:9251
24. Sljukic B, Banks CE, Compton RG (2006) Nano Lett 6:1556
25. Savinova ER, Wasle S, Doblhofer K (1998) Electrochim Acta 44:1341
26. Karyakin AA, Puganova EA, Budashov IA, Kurochkin IN, Karyakina EE, Levchenko VA, Matveyenko VN, Varfolomeye SD (2004) Anal Chem 76:474
27. You T, Niwa O, Tomita M, Hirono S (2003) Anal Chem 75:2080
28. Kim J, Gewirth AA (2005) J Phys Chem B 109:9684
29. Maduraiveeran G, Ramaraj R (2007) J Electroanal Chem 608:52
30. Abdel Haleem SM, Ateya BG (1981) J Electroanal Chem 117:309
31. Burke LD, Bruton GM, Collins JA (1998) Electrochim Acta 44:1467
32. Vazquez MV, de Sanchez SR, Calvo EJ, Schiffrin DJ (1994) J Electroanal Chem 374:179

33. Delahay P (1950) J Electrochem Soc 97:205
34. Calvo EJ, Schiffrin DJ (1988) J Electroanal Chem 243:171
35. Burke LD, Sharna R (2007) J Appl Electrochem 37:1119
36. Scharifker B, Hills G (1983) Electrochem Acta 28:879
37. Sarkar DK, Zhou XJ, Tannous A, Leung KT (2003) J Phys Chem B 107:2879
38. Macdonald JR (1987) Impedance spectroscopy emphasizing solid materials and systems. Wiley, New York
39. Bard AJ, Faulkner LR (1980) Electrochemical methods: fundamentals and applications. Wiley, New York
40. Wang J, Wang L, Liu S (2003) Biophys Chem 106:31
41. Zen J-M, Chung H-H, Kumar AS (2000) Analyst 125:1633
42. Burke LD, O'Connell AM, Sharna R, Buckley CA (2006) J Appl Electrochem 36:919
43. Murray RW (1984) In: Bard AJ (ed) Electroanalytical chemistry, vol 13. Dekker, New York
44. Taniguchi I (1997) Electrochem Soc Interface 6:34
45. Selvaraju T, Ramaraj R (2007) Electrochim Acta 52:2998